Engineering Science and Technology, an International Journal xxx (2016) xxx–xxx

HOSTED BY

Contents lists available at ScienceDirect

Engineering Science and Technology, an International Journal

journal homepage: www.elsevier.com/locate/jestch

Full Length Article

# Artificial Neural Network model for the determination of GSM Rxlevel from atmospheric parameters

Eichie Julia Ofure [a,*], Oyedum Onyedi David [a], Ajewole Moses Oludare [b], Aibinu Abiodun Musa [c]

[a] Department of Physics, Federal University of Technology, Minna, Nigeria
[b] Department of Physics, Federal University of Technology, Akure, Nigeria
[c] Department of Mechatronics Engineering, Federal University of Technology, Minna, Nigeria

ARTICLE INFO

*Article history:*
Received 2 August 2016
Revised 25 October 2016
Accepted 3 November 2016
Available online xxxx

*Keywords:*
Artificial Neural Network
Dew point
Relative humidity
Rxlevel
Temperature

ABSTRACT

Accurate received signal level (Rxlevel) values are useful for mobile telecommunication network planning. Rxlevel is affected by the dynamics of the atmosphere through which it propagates. Adequate knowledge of the prevailing atmospheric conditions in an environment is essential for proper network planning. However most of the existing GSM received signal determination model are function of distance between point of signal reception and transmitting site thus necessitating the development of a model that involve the use of atmospheric parameters in the determination of received GSM signal level. In this paper, a three stage approach was used in the development of the model using some atmospheric parameters such as atmospheric temperature, relative humidity and dew point. The selected and easily measurable atmospheric parameters were used as input parameters in developing two new models for computing the Rxlevel of GSM signal using a three-step approach. Data acquisition and pre-processing serves as the first stage and formulation of ANN design and the development of parametric model for the Rxlevel using ANN synaptic weights form the second stage of the proposed approach. The third stage involves the use of ANN weight and bias values, and network architecture in the development of the model equation. In evaluating the performance of the proposed models, network parameters were varied and the results obtained using mean squared error (MSE) as performance measure showed the developed model with 33 neurons in the hidden layer and tansig activation, function in both the hidden and output layers as the optimal model with least MSE value of 0.056. Thus showing that the developed model has an acceptable accuracy value as demonstrated from comparison of results with actual measured values.


## 1. Introduction

Empirical models are used in the planning of mobile communication networks. Due to the differences in environmental structures, local terrain profiles and weather conditions, the signal strength and path loss prediction model for a given environment, with reference to existing empirical models, often differ from the optimal model. Accurate signal strength values are necessary for network planning. Mobile telecommunications depend on the propagation of radio waves within the troposphere, the region of the atmosphere extending from the Earth's surface up to an altitude of about 16 km at the equator or 8 km at the poles [1]. Propagation of radio waves through space is governed to a great degree by the dynamics and physical properties of the atmosphere and objects in the propagation path. Environmental, atmospheric and climatic conditions impair Global System for Mobile Communication (GSM) signal propagation and may result in reduction of the strength of received signal and deformation of signal quality over time. The environmental and weather effects on signal strength need to be properly understood in given environments to enhance optimal planning of such networks.

The Earth's weather system is confined to the troposphere and the fluctuations in weather parameters like temperature, pressure and humidity within the atmospheric layer cause the refractive index of the air in this layer to vary from one location to another and from time to time. The variation in the refractive index of the atmosphere results in various degrees of refraction of mobile signals. Under abnormal conditions such as ducting, the signal strength can also be enhanced and this enables the signals to reach unintended locations where they may constitute interference to

* Corresponding author.
*E-mail addresses:* juliaeichie@futminna.edu.ng (J.O. Eichie), onyedidavid@futminna.edu.ng (O.D. Oyedum), oludare.ajewole@futa.edu.ng (M.O. Ajewole), abiodun.aibinu@futminna.edu.ng (A.M. Aibinu).

Peer review under responsibility of Karabuk University.

http://dx.doi.org/10.1016/j.jestch.2016.11.002
2215-0986/

Please cite this article in press as: J.O. Eichie et al., Artificial Neural Network model for the determination of GSM Rxlevel from atmospheric parameters, Eng. Sci. Tech., Int. J. (2016), http://dx.doi.org/10.1016/j.jestch.2016.11.002

other co-channel networks. The refractive properties of the troposphere is expressed by the radio refractivity, N, given by

$$N = (n - 1) \times 10^6 \quad (1)$$

where n = refractive index of air. N depends on meteorological factors of air pressure, P (hPa), air temperature, t (°C) and water vapour pressure, e (hPa), which are related to N as [2]:

$$N = 77.6\left(\frac{P}{T}\right) + 3.732 \times 10^5\left(\frac{e}{T^2}\right) \quad (2)$$

where T(K) = t + 273, and

$$e = \frac{He_s}{100} \quad (3)$$

where e is water vapour pressure, H is relative humidity, and $e_s$ the saturated water vapour pressure given as:

$$e_s = 6.11\exp\left(\frac{17.502t}{T}\right) \quad (4)$$

Surface refractivity, $N_s$, is known to have high correlation with radio field strength values [3,4] and seasonal variations in $N_s$ have been found to agree in general with the observations of the variation of radio field strength at VHF and UHF in Nigeria [5,6]. Thus, surface radio refractivity is a function of atmospheric parameters of temperature, pressure and relative humidity near the surface.

Temperature and relative humidity have been found to have some correlation with GSM Rxlevel [7,8,9]. Zilinskas et al. [10] showed that there is no obvious correlation between atmospheric pressure and received signal strength. Some relationships exist between atmospheric temperature, relative humidity and dew point. Atmospheric temperature is the degree of hotness or coldness of the atmosphere. Humidity is a measure of the quantity of water vapour or the gaseous state of water, in the atmosphere, and is usually invisible. The maximum amount of water vapour in the atmosphere depends on the atmospheric temperature [9]. Relative humidity (RH) defines the amount of water vapour in the atmosphere relative to the maximum amount of water vapour the air can take at the same atmospheric temperature and pressure. Relative humidity of the saturated atmosphere is 100% and as atmospheric water vapour increases towards saturation point, atmospheric temperature decreases. In other words, relative humidity is inversely proportional to atmospheric temperature. Dew point is the temperature to which the atmosphere must be cooled to enable water vapour condense into liquid water or ice (RH = 100%). Relative humidity and dew point are both reflection of the amount of water vapour in the atmosphere. Each of them is also a function of temperature. Thus, relative humidity, temperature and dew point are interrelated and their relationship with radio field strength makes them reliable as inputs in received signal level computation model. Artificial Neural Network has been found to be very effective in prediction problems and useful in the development of models [11].

Artificial Neural Network (ANN) is one of the artificial intelligence techniques. It is based on understanding the structure and function of the physical biological neurons of the human brain and the ability of the human brain to learn through example [12]. ANN has proven to be flexible and with capability to learn the underlying relationships between the inputs and outputs of a process, without needing the explicit knowledge of how these variables are related [13]. ANN can learn, adapt, predict and classify. In this study, the atmospheric parameters such as temperature, relative humidity and dew point that have been found to have relationship with the temporal variation of GSM Rxlevel were used to develop a model that computes GSM Rxlevel. This is useful for determining coverage areas of base stations, frequency assignments, interference analysis, handover optimisation, optimal transmitting antenna height and power level adjustment.

There is need for the determination of propagation characteristics of given environments, especially in tropical regions of Africa, as requested by ITU-R. Acquisition of empirical signal field strength data could be difficult, due to paucity of relevant equipment. But acquisition of atmospheric data is relatively cheaper and the data are more available.

The rest of this paper is organized as follows: Section 2 presents literature review while Section 3 presents model design and development. Results and discussion is presented in Section 4 while conclusion is in Section 5.

## 2. Literature review

This section is divided into two sub-sections. In subsection 2.1, review of recently published related work from literature have been undertaken while in subsection 2.2 an overview into ANN which is used in Section 3 in the developing of the appropriate model has been provided.

### 2.1. Related field Measurements and ANN Applications

Adewumi *et al.* [8] studied the influence of atmospheric parameters on UHF Radio Propagation in South Western Nigeria. Received signal level was observed to increase with increase in temperature while relative humidity increased with signal path loss. The study revealed that air temperature and relative humidity have significant influence on UHF signal propagation within the tropospheric region of southwest Nigeria. Zilinskas *et al.* [10] investigated the influence of atmospheric radio refractivity on WiMax signal level. The study revealed that atmospheric radio refractivity, as a combination of temperature and relative humidity, has impact on the variation of received signal level. Increase in refractivity values had a corresponding decrease in received signal level.

Famorji *et al.* [14] revealed an inverse relationship between atmospheric radio refractivity and UHF received signal level with correlation coefficient value of −0.97. The study also revealed a direct relationship between atmospheric radio refractivity and relative humidity and an inverse relationship between atmospheric radio refractivity and temperature. Sheowu and Akinyemi [15] investigated the effect of climatic change on GSM signal propagation by sampling the three ITU regions in Nigeria at different climatic seasons of rain (May–June) and harmattan (November–March). The result obtained revealed that climate affects signal propagation.

Afrand *et al.* [16] developed an optimal Artificial Neural Network to predict the thermal conductivity ratio of the magnetic nanofluid and Afrand *et al.* [17] predicted dynamic viscosity of a hybrid nano-lubricant using an optimal Artificial Neural Network. Comparison of the experimental data, empirical correlation and the optimal ANN outputs showed that the optimal Artificial Neural Network model is more accurate. Philippopoulos and Deligiorgi [18] assessed the spatial predictive ability of ANNs to estimate mean hourly wind speed values in Chania City, Greece. The predicted values were compared with five traditional spatial interpolation schemes and ANNs were observed to efficiently predict the mean wind speed spatial variability in Chania City.

Esfe *et al.* [19] applied feedforward multilayer perceptron Artificial Neural Networks and empirical correlation, for the prediction of thermal conductivity of $Mg(OH)_2$–EG using experimental data. The results of the developed models revealed that, in the absence of costly and time-consuming tests, the impact of temperature and volume fraction on $Mg(OH)_2$–EG nanofluids' thermal

Please cite this article in press as: J.O. Eichie et al., Artificial Neural Network model for the determination of GSM Rxlevel from atmospheric parameters, Eng. Sci. Tech., Int. J. (2016), http://dx.doi.org/10.1016/j.jestch.2016.11.002

conductivity can be analyzed with ANN models. Litta *et al.* [20] evaluated the utility of multilayer perceptron network (MLPN) ANN model for the prediction of hourly surface temperature and relative humidity in Kolkata, India. The study showed that ANN models were capable of predicting hourly temperature and relative humidity adequately and the developed ANN models were applied in the prediction of thunderstorm in Kolkata.

### 2.2. Overview of ANN

ANN is an information processing system constituted by an assembly of a large number of simple processing elements that are interconnected to perform a parallel distributed processing in order to solve specific task, such as pattern classification, function approximation, clustering (or categorisation), prediction (forecasting or estimation), optimisation and control [13]. The Process Elements (PEs) attempt to simulate the structure and function of the physical biological neurons of the human brain. The fundamental principle of ANN is based on finding coefficients between the inputs and outputs of a problem, making connections between input and output layers and performing operations on a learning system [21]. The fundamental element of ANN is the neuron. Each neuron handles:

i. the multiplication of the network inputs, $x_1$, $x_2$, $x_3$, ...$x_n$ (from original data, or from the output of other neurons in a neural network) by the associated input weights,
ii. the summation of the weight and input product to the bias value associated with the neuron, and
iii. the passage of the summation result, $u$, through a linear or nonlinear transformation called the activation function, $\varphi$. The neuron's output, $y$, is the result of the action of the activation function.

$$\varphi = f(u) \tag{5}$$

$$y = \varphi\left(\sum_{i=1}^{n} x_i w_i + b\right) \tag{6}$$

$$y = \varphi(w^T x + b) \tag{7}$$

where $b$ is the bias value (or external threshold), $w_i$, is the weight of the respective inputs $x_i$, $u$ is the argument of the activation function and $w^T$ is a transpose of the weight vector.

The weight and bias are adjustable parameters of the neuron that causes the network to exhibit some desired or interesting behaviours. Fig. 1 shows an illustration of an artificial neuron.

ANN architecture can be classified into two main topologies: feed-forward multilayer networks and feedback recurrent networks. In the former network, feedback connections are not allowed while loops and iteration for a potentially long time before producing a response exist in the latter. The most commonly used type of feed-forward network is the multilayer perceptron [22]. A multilayer perceptron (MLP) network consists of a set of input nodes, one or more hidden layers and a set of output nodes in the output layer. MLP network has the ability to model simple and as well as complicated functional relationships.

## 3. Model design and development

In this section, the design and development of the ANN model for determination of Rxlevel is presented. The proposed approach involves a three stage approach namely, data collection and pre-processing, network design and model development. Detailed information about each of the aforementioned stages is provided herewith.

### 3.1. Data collection and pre-processing

Twelve months (June 2014 to May 2015) atmospheric data were acquired from the Nigeria Environmental and Climate Observation Programme (NECOP) weather station at the Bosso Campus of the Federal University of Technology, Minna, Nigeria. Concurrently, the GSM Rxlevel of Mobile Telecommunications Network (MTN) with the frequency band 1835–1850 MHz was measured using a spectrum analyser (SPECTRAN HF 6065) connected to a laptop loaded with Aarisona data logging software. Figs. 2 and 3 show the NECOP weather station and the GSM Rxlevel measurement setup used in this study.

The atmospheric data and GSM Rxlevel were measured at 5 min and 500 ms intervals respectively, GSM Rxlevel data were averaged to 5 min intervals for each day of the 12 months. The missing data in the input data (atmospheric temperature, relative humidity and dew point data) and the output data (GSM Rxlevel data) were replaced by the average of neighbouring values. The terrain of the propagation environment is relatively flat and unpaved. There are farm lands, vegetation cover, few trees and bungalow buildings between the transmitting and the measurement sites. The physical profile of the fixed wireless link consisting of the MTN base station and the measurement site is shown in Fig. 4.

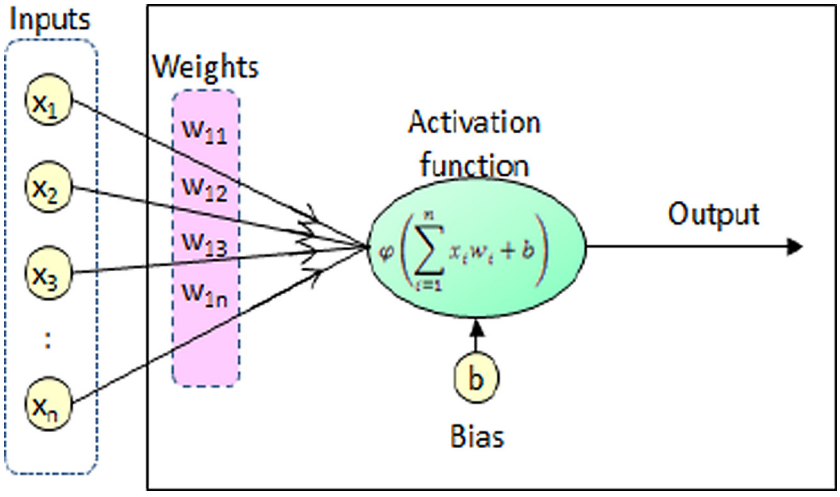


**Fig. 1.** Artificial Neuron.

Please cite this article in press as: J.O. Eichie et al., Artificial Neural Network model for the determination of GSM Rxlevel from atmospheric parameters, Eng. Sci. Tech., Int. J. (2016), http://dx.doi.org/10.1016/j.jestch.2016.11.002

(a) A view of the Weather Station (b) Downloading of Atmospheric Data to a laptop

**Fig. 2.** The NECOP Weather Station.

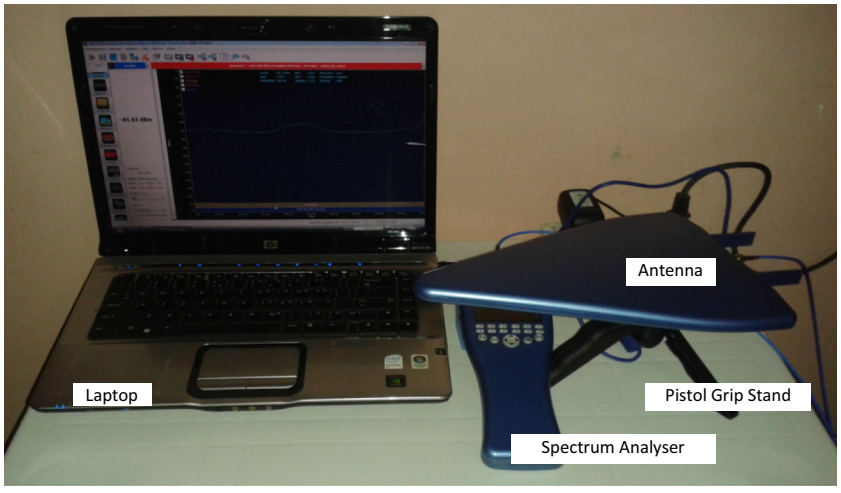


**Fig. 3.** Spectran HF 6065 and a Laptop for Data Logging.

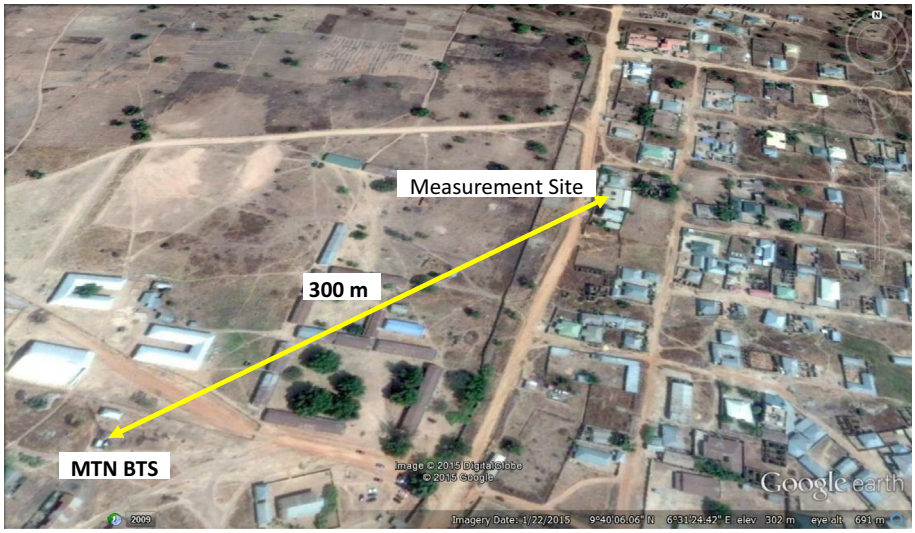


**Fig. 4.** Physical Profile of the Fixed Wireless Link (Google Earth).

Please cite this article in press as: J.O. Eichie et al., Artificial Neural Network model for the determination of GSM Rxlevel from atmospheric parameters, Eng. Sci. Tech., Int. J. (2016), http://dx.doi.org/10.1016/j.jestch.2016.11.002

### 3.2. Design of ANN based Rxlevel determination model

The proposed MLP network consists of 3 nodes at the input layer, one hidden layer and 1 node at the output layer. In the proposed model, 3 most frequently used activation functions have been considered [23]. These are:

i. Logistic sigmoid activation function also known as logsig.

$$f(u) = \frac{1}{1+e^{-u}} \tag{8}$$

ii. Hyperbolic tangent sigmoid activation function also known as tansig.

$$f(u) = \frac{2}{1+e^{-2u}} - 1 \tag{9}$$

iii. Linear activation function also known as purelin.

$$f(u) = u \tag{10}$$

A schematic of the proposed MLP network with variable neurons in the hidden layer is shown in Fig. 5.where $x_i$ (where $1 \leqslant i \geqslant 3$) are the set of inputs; $w_{ij}$ and $w_{jk}$ are adjustable weight values: $w_{ij}$ connects the *ith* input to the *jth* neuron in the hidden layer, $w_{jk}$ connects the *jth* output in the hidden layer to the *kth* node in the output layer; $y_k$ (where $k = 1$) is the output. Each neuron and output node has associated adjustable bias values: $b_j$ (where j = number of neurons) is associated with the *jth* neuron in network layer 1, $b_k$ (where $k = 1$) is associated with the node in the network layer 2. Within each network layer are: the weights, *w*, the multiplication and summing operations, the bias, *b*, and the activation function, φ [23,24]. Mathematically, Fig. 5 can be represented as:

$$y_l = \varphi_2\left(\sum_{j=1}^{m} w_{j1}\,\varphi_1\left(\sum_{i=1}^{3} w_{ij}x_i + b_j\right) + b_1\right) \tag{11}$$

where *m* is the total number of neurons in the hidden layer. The operations within an *N* layered MLP network can be mathematically represented by;

$$y_l = \underbrace{\varphi_N\left(\sum_{l=1}^{p} w_{kl} \ldots \underbrace{\varphi_2\left(\sum_{j=1}^{m} w_{jk}\,\underbrace{\varphi_1\left(\sum_{i=1}^{n} w_{ij}x_i + b_j\right)}_{layer\ 1} + b_k\right)}_{layer\ 2} + \ldots\ldots + b_l\right)}_{\substack{\vdots \\ layer\ N}} \tag{12}$$

where *l* is the number for the *lth* neuron in layer *N*, *p* is the maximum number of neurons in layer *N* and *N* is the total number of network layers.

For linear activation function in both hidden and output layers and the use of *m* number of neurons in the hidden layer, Eq. (11) is transformed into:

$$y = LW[IW * X + b_1] + b_2 \tag{13}$$

$$y = [LW * IW] * X + [LW * b_1] + b_2 \tag{14}$$

where

Layer weights, LW = [1,m] matrix
Input weights, IW = [m,3] matrix
Layer 1 bias, $b_1$ = [m,1] matrix
Layer 2 bias, $b_2$ = *c*
Input vector, X = [3,1] matrix

Thus,

$$[LW * IW] = [\alpha\,\beta\,\gamma] \tag{15}$$

$$[LW * IW] * X = [\alpha\,\beta\,\gamma]\begin{bmatrix} T \\ R \\ D \end{bmatrix} \tag{16}$$

The proposed model equation is:

$$y = \alpha T + \beta R + \gamma D + c \tag{17}$$

Similarly, adopting the same approach for tansig activation function, another proposed model equation for the determination

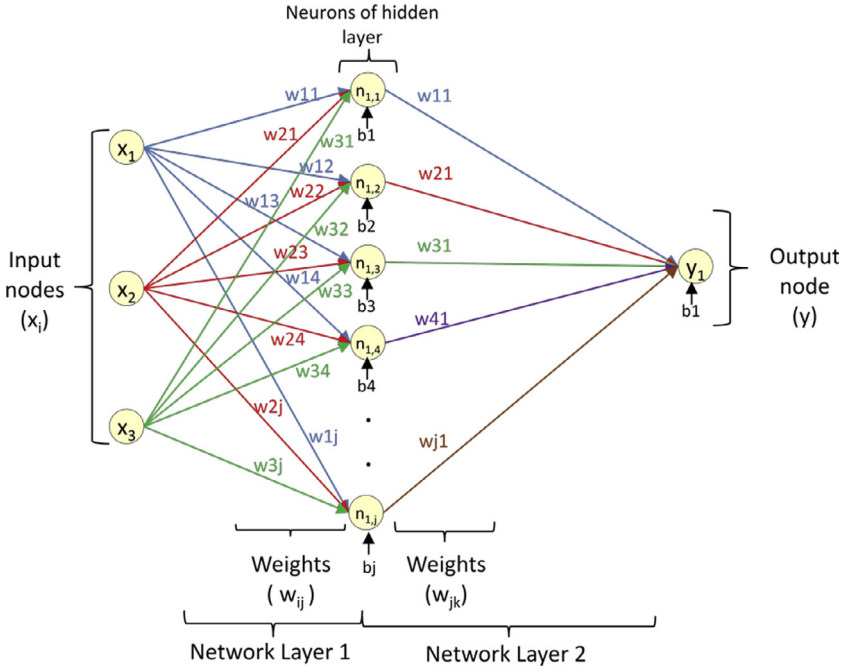


**Fig. 5.** A 2 layered MLP network.

Please cite this article in press as: J.O. Eichie et al., Artificial Neural Network model for the determination of GSM Rxlevel from atmospheric parameters, Eng. Sci. Tech., Int. J. (2016), http://dx.doi.org/10.1016/j.jestch.2016.11.002

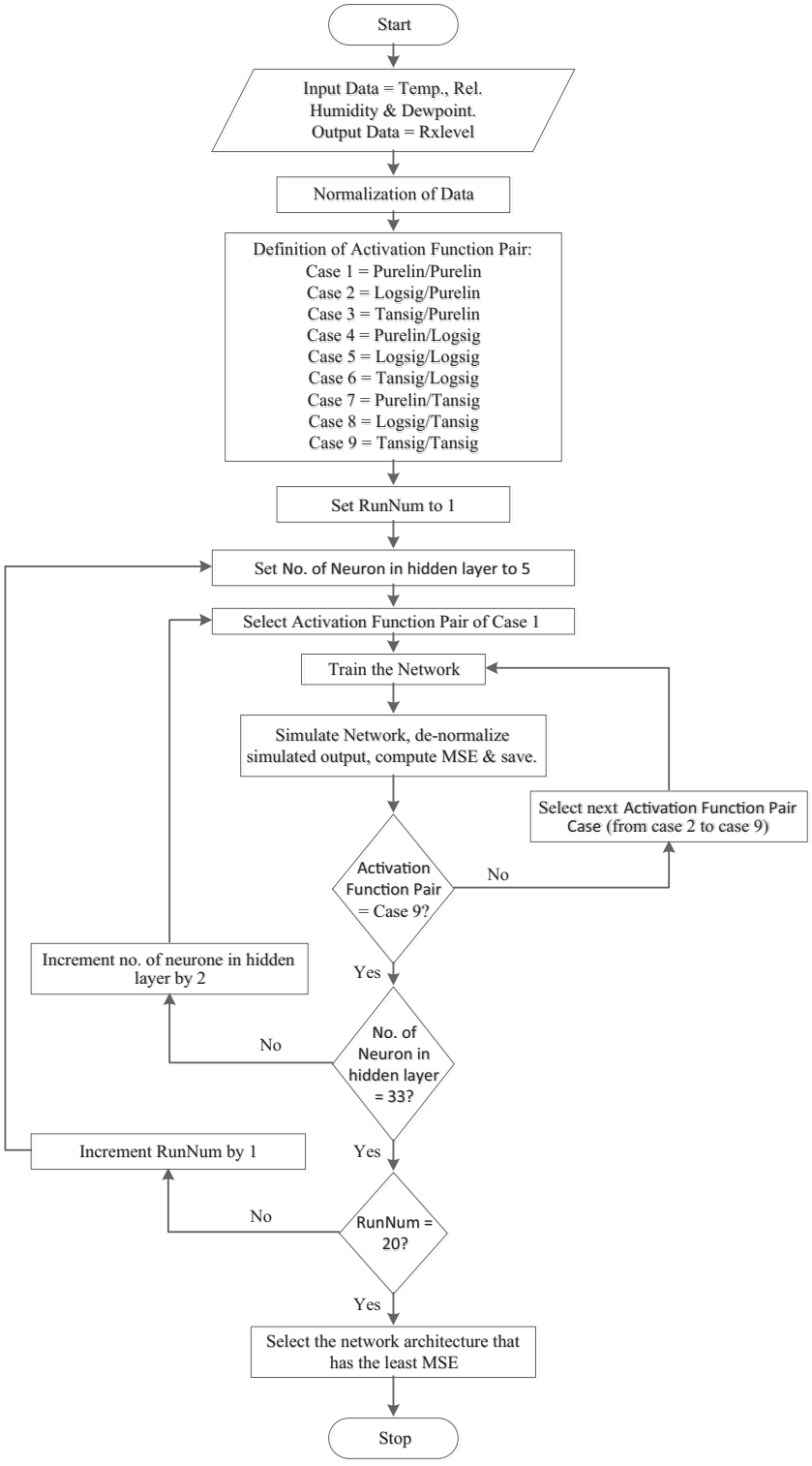


**Fig. 6.** Flow Diagram of the ANN Script.

of GSM Rxlevel, using atmospheric temperature, relative humidity and dew point as independent variables can be expressed as:

$$y = \frac{2}{1+\exp\left(-2\left(\alpha\left(\frac{2}{1+\exp(-2(\beta x+b))}-1\right)+c\right)\right)}-1 \quad (18)$$

where $x$ is the input vector of atmospheric temperature, relative humidity and dew point, $\alpha$, $\beta$, $b$ and $c$ are constant values.

### 3.3. Model development

MATLAB was used to write the script files for the developed Rxlevel determination model and performance analysis to determine the weight and bias values, number of neurons and activation function type to be used in the optimal model equation. The script files were written to compare the relative effect of number of hidden layer neurons and activation function type on the performance

Please cite this article in press as: J.O. Eichie et al., Artificial Neural Network model for the determination of GSM Rxlevel from atmospheric parameters, Eng. Sci. Tech., Int. J. (2016), http://dx.doi.org/10.1016/j.jestch.2016.11.002

of a designed network. A feedforward network topology and the default Matlab Neural Network Toolbox learning algorithm, Levenberg–Marquardt, were used. The number of neurons in the hidden layer was varied from 5 to 33 in incremental steps of 2. Logsig, purelin and tansig type of activation functions were used to create 9 different pairs of activation functions. Thus, each of the 15 different numbers of neurons was used with 9 different pairs of activation functions. Each run of the script file generates 135 networks.

For networks in which activation function pairs with logsig or tansig functions were used in the output layer, the input and target output data were pre-processed into 0–1 or −1 to +1 range using Eqs. (19) and (20) respectively.

$$X_{norm\_0\_1} = \frac{X - X_{min}}{X_{max} - X_{min}} \tag{19}$$

$$X_{norm\_-1\_1} = 2 \times \frac{X - X_{min}}{X_{max} - X_{min}} - 1 \tag{20}$$

The network outputs from the simulation process were then post processed to the original range. To compare the relative effect of number of runs on network performance, the script file was run 20 times and 20 runs generated 2700 trained networks for performance evaluation. The flow diagram of the ANN script file is shown in Fig. 6.

Out of the 12 months data (3465 samples), 864 samples were used while training the network. During the training process, the input and target output data were applied to the network and the network computed its output. The initial weight and bias values and their subsequent adjustments were done by the Matlab Neural Network Toolbox software. For each set of output in the output data, the error, *e*, (the difference between the target output, *t*, and the network's output, *y*,) was computed. The computed errors were used by the network performance function to optimize the network and the default network performance function for feedforward networks is mean squared error, *MSE* (the mean of the sum of the squared errors) which is given by:

$$MSE = 1/N\left(\sum_{i=1}^{N}(e_i)^2\right) \tag{21}$$

$$MSE = 1/N\left(\sum_{i=1}^{N}(t_i - y_i)^2\right) \tag{22}$$

where N is the number of sets in the output data. The weight and bias values are adjusted so as to minimize the mean squared error and thus increase the network performance. After the adjustments, the network undergoes a retraining process, the mean square error is recomputed and the weight and bias values are readjusted. The retraining continues until the training data achieves the desired mapping to obtain minimum mean square error value.

## 4. Results and discussion

The performances of the developed ANN based Rxlevel models were evaluated using *MSE*. For each of the activation function pair, the best and worst performed networks in the 20 run of the script file were determined with the least and highest MSE value. Tables 1 and 2 show the performance comparison of the best and worst networks for each of the 9 pairs of activation function.

As can be seen from Tables 1 and 2, the number of run of the script file has no obvious effect on the performance of the trained

**Table 1**
Best Performance in 20 Runs for 9 Pairs of Activation Function.

| Hidden Layer | Output Layer | No. of Runs | No. of Neurons in hidden layer | MSE |
|---|---|---|---|---|
| Purelin | Purelin | 6 | 5 | 0.5084 |
| Purelin | Tansig | 16 | 15 | 0.5118 |
| Purelin | Logsig | 5 | 15 | 0.5118 |
| Logsig | Purelin | 5 | 31 | 0.1270 |
| Logsig | Tansig | 14 | 33 | 0.0602 |
| Logsig | Logsig | 20 | 33 | 0.0615 |
| Tansig | Tansig | **14** | **33** | **0.0566** |
| Tansig | Logsig | 7 | 33 | 0.0651 |
| Tansig | Purelin | 9 | 31 | 0.0995 |

**Table 2**
Worst Performance in 20 Runs for 9 Pairs of Activation Function.

| Hidden Layer | Output Layer | No. of Runs | No. of Neurons in hidden layer | MSE |
|---|---|---|---|---|
| Purelin | Purelin | 3 | 17 | 0.5084 |
| | | 8 | 11 | 0.5084 |
| Purelin | Tansig | 18 | 15 | 0.5118 |
| Purelin | Logsig | **6** | **19** | **2.5329** |
| | | **8** | **21** | **2.5329** |
| | | **7** | **27** | **2.5329** |
| Logsig | purelin | 2 | 9 | 0.5211 |
| Logsig | Tansig | **18** | **11** | **2.5329** |
| | | **19** | **17** | **2.5329** |
| | | **8** | **21** | **2.5329** |
| Logsig | Logsig | **1** | **11** | **2.5329** |
| | | **10** | **15** | **2.5329** |
| Tansig | Purelin | 4 | 5 | 0.7165 |
| Tansig | Tansig | **7** | **9** | **2.5329** |
| | | **12** | **13** | **2.5329** |
| | | **17** | **17** | **2.5329** |
| Tansig | Logsig | **10** | **9** | **2.5329** |
| | | **13** | **19** | **2.5329** |
| | | **8** | **21** | **2.5329** |

The number of runs, number of neurons in the hidden layer and the MSE values of the worst performed networks are shown in bold font.

Please cite this article in press as: J.O. Eichie et al., Artificial Neural Network model for the determination of GSM Rxlevel from atmospheric parameters, Eng. Sci. Tech., Int. J. (2016), http://dx.doi.org/10.1016/j.jestch.2016.11.002

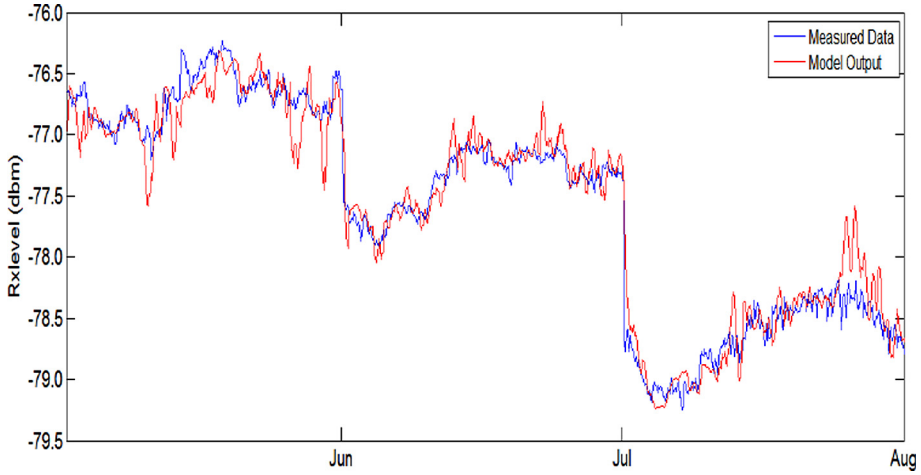


**Fig. 7.** Comparison of Measured Rxlevel and Model Predicted Rxlevel.

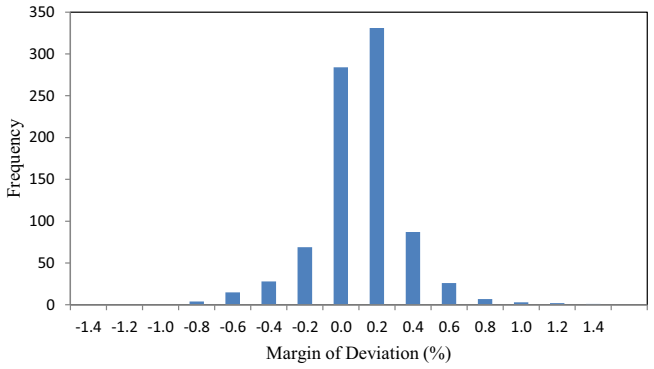


**Fig. 8.** Histogram of Margin of Deviation for Model Predicted Rxlevel.

network. Increasing the number of neurons in the hidden layer for networks with logsig or tansig activation function in the hidden layer, decreases the MSE value and thus increases the network performance. But for networks with purelin activation function in the hidden layer, increasing the number of neurons has no obvious effect on the network performance. In Table 1, the best performed network had least MSE value of **0.0566** at the **14th** run of the script file with the use of **33** neurones in the hidden layer. 14 networks had the worst performance with highest MSE value of 2.5329. Activation function pairs of tansig/tansig, tansig/logsig, logsig/tansig and logsig/logsig performed worst with low number of neurons in the hidden layer.

Using the weight and bias values, the architecture of the network, for linear activation function in the hidden and output layers [25], the proposed model Eq. (17) for the computation of GSM Rxlevel, using atmospheric temperature, relative humidity and dew point is transformed into the model equation:

$$y = 0.2467T + 0.0167R + 0.0657D + 105.303 \tag{23}$$

where T = temperature, R = relative humidity and D = dew point. Similarly, for tansig activation function, Eq. (19) is transformed into the model equation:

$$y = \frac{2}{1+\exp\left(-2\left(\alpha\left(\frac{2}{1+\exp(-2(\beta x+b))}-1\right)-2.9156\right)\right)}-1 \tag{24}$$

where x is the input vector of atmospheric temperature, relative humidity and dew point, α, β, and b are constant values.

The network architecture of 3-33-1, with tansig/tansig pair of activation functions performed best with least MSE value of 0.0566. Using the weight and bias values, and the architecture of the network with the best performance, the optimal model equation developed for the computation of GSM Rxlevel using atmospheric parameters such as atmospheric temperature, relative humidity and dew point is Eq. (25).

The deviations between the measured Rxlevels and the model predicted Rxlevels were computed using Eq. (26) and were used in deviation analysis of the developed optimal model to evaluate its accuracy.

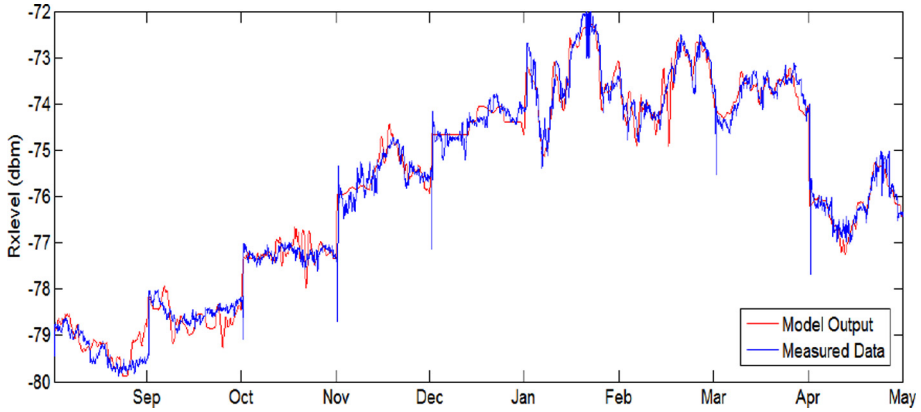


**Fig. 9.** Testing of Model on 2592 samples (September to May data) of Atmospheric Data.

Please cite this article in press as: J.O. Eichie et al., Artificial Neural Network model for the determination of GSM Rxlevel from atmospheric parameters, Eng. Sci. Tech., Int. J. (2016), http://dx.doi.org/10.1016/j.jestch.2016.11.002

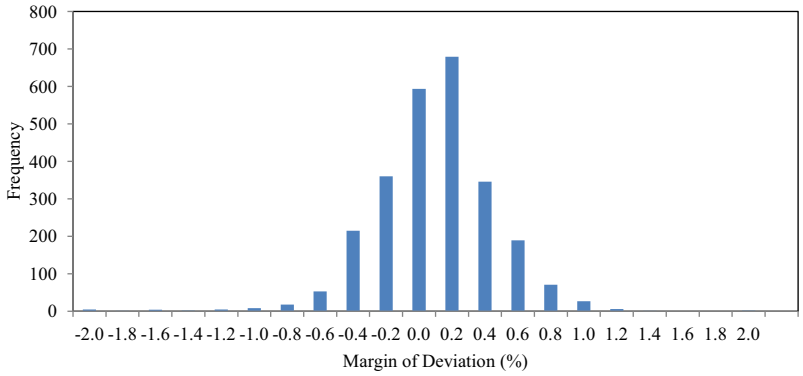


**Fig. 10.** Histogram of Margin of Deviation for Model Predicted Rxlevel when Tested on 2592 Samples.

$$\text{Margin of deviation} = \left[\frac{y_m - y_p}{y_m}\right] \times 100 \quad (25)$$

where $y_m$ = measured Rxlevel and $y_p$ = model predicted Rxlevel. The model was used on 2592 samples (September to May data). Comparison was made between the measured Rxlevels and the model predicted Rxlevels.

Fig. 7 shows plots of measured Rxlevels and model predicted Rxlevels, and histogram of the margin of deviation for the model predicted Rxlevel is shown in Fig. 8.

The measured Rxlevel and model determined Rxlevel had correlation value of 0.706 when computed with Pearson correlation coefficient formula:

$$r = \frac{n(\sum xy) - (\sum x)(\sum y)}{\sqrt{[n\sum x^2 - (\sum x)^2][n\sum y^2 - (\sum y)^2]}} \quad (26)$$

where

r = Pearson correlation coefficient
x = values in first set of data
y = values in second set of data
n = total number of values

Fig. 8 shows that the deviation distribution is concentrated around 0 and this conotes acceptable accuracy of the model [17]. Result obtained from the use of the model on 2592 samples (September to May data) is shown in Fig. 9 and the computed correlation coefficient value was 0.906. The histogram of margin of deviation shown in Fig. 10, shows that the developed model has an acceptable accuracy.

## 5. Conclusion

In this study atmospheric temperature, relative humidity and dew point, were used as inputs in the development of ANN based Rxlevel determination parametric model for the determination of received GSM signal level. Network parameters such as number of neurons in the hidden layer and activation function were varied during the performance evaluation process. The use of Levenberg-Marquard algorithm, network architecture of 3-33-1, tansig activation function in both the hidden layer and output layer was the optimal combination that gave the best performance with least MSE value of 0.056. The weight and bias values and the architecture of the MLP network were used in the development of a model equation. Comparisons of the measured and model output, showed that the developed model can efficiently determine the GSM Rxlevel using atmospheric temperature, relative humidity and dew point as input parameters.

## Funding

This research did not receive any specific grant from funding agencies in the public, commercial, or not-for-profit sectors.

## Acknowledgment

The data used in this paper were obtained from the NECOP weather station in the Bosso campus of the Federal University of Technology, Minna, Nigeria and it was provided by the Centre for Basic Space Science, University of Nigeria, Nsukka. The authors are grateful to the centre for providing the weather station.

## References

[1] B.M. Reddy, Physics of the Troposphere, in: Handbook on Radio Propagation for Tropical and Subtropical Countries, URSI committee on developing countries, UNESCO subvention, New Delhi, 1987, pp. 59–77.
[2] E.K. Smith, S. Weintraub, 1953, Proceedings of the Institute of Radio Engineers (IRE), 41, 1035
[3] B.R. Bean, B.A. Cohoon, Correlation of monthly median transmission loss and refractive index profile characteristics, J. Res. Nat. Bur. Stand. 65D (1) (1961) 67–74.
[4] M.P. Hall, Effects of the Troposphere on Radio Communications, Peter Peregrinus, 1979.
[5] I.E. Owolabi, V.A. Williams, Surface radio refractivity patterns in Nigeria and the Southern Cameroon, J. West Afr. Sci. Assoc. 15 (1970) 3–17.
[6] O.D. Oyedum, G.K. Gambo, Surface radio refractivity in Northern Nigeria, Niger. J. Phys. 6 (1994) 36–41.
[7] A.U. Usman, O.U. Okereke, E.E. Omizegba, Instantaneous GSM signal strength variation with weather and environmental factors, Am. J. Eng. Res. (AJSER) 4 (3) (2015) 104–115.
[8] A.S. Adewumi, M.O. Alade, H.K. Adewumi, Influence of air temperature, relative humidity and atmospheric moisture on UHF radio propagation in South Western Nigeria, Int. J. Sci. Res. (IJSR) 4 (8) (2015) 588–592.
[9] J. Luomala, I. Hakala, Effects of temperature and humidity on radio signal strength in outdoor wireless sensor networks, Proc. Federated Conf. Comput. Sci. Inf. Syst. 5 (2015) 1247–1255.
[10] M. Zilinskas, M. Tamosiunaite, S. Tamosiunas, M. Tamosiuniene, E. Stankevicius, 2015, The infuence of atmospheric radio refractivity on the WiMAX signal level in the areas of weak coverage, progress In: Electromagnetics Research Symposium Proceedings, Prague, Czech Republic, pp. 580–584.
[11] M. Afrand, A.A. Nadooshan, M. Hassani, H. Yarmand, M. Dahari, Predicting the viscosity of multi-walled carbon nanotubes/water nanofluid by developing an optimal artificial neural network based on experimental data, Int. Commun. Heat Mass 77 (2016) 49–53.
[12] H. Elçiçek, E. Akdoğan, S. Karagöz, The use of artificial neural network for prediction of dissolution kinetics, Sci. World J. 2014 (2014) 1–9.
[13] D. Deligiorgi, K. Philippopoulos, G. Kouroupetroglou, Artificial neural network based methodologies for the spatial and temporal estimation of air temperature, Int. Conf. Pattern Recognit. Appl. Methods (2013) 669–678.
[14] J.O. Famorji, M.O. Oyeleye, A test of the relationship between refractivity and radio signal propagation for dry particulates, Res. Desk 2 (4) (2013) 334–338.
[15] O. Sheowu, L.A. Akinyemi, Effect of climatic change on GSM signal, Res. J. Comput. Syst. Eng. – RJCSE 4 (2) (2013) 471–478.
[16] M. Afrand, D. Toghraie, N. Sina, Experimental study on thermal conductivity of water-based $Fe_3O_4$ nanofluid: development of a new correlation and modeled by artificial neural network, Int. Commun. Heat Mass 75 (2016) 262–269.

[17] M. Afrand, K.N. Najafabadi, N. Sina, M.R. Safaei, A.S. Kherbeet, S. Wongwises, M. Dahari, Prediction of dynamic viscosity of a hybrid nano-lubricant by an optimal artificial neural network, Int. Commun. Heat Mass Transfer 76 (2016) 209–214.

[18] K. Philippopoulos, D. Deligiorgi, Application of artificial neural networks for the spatial estimation of wind speed in a coastal region with complex topography, Renew. Energ. 38 (2012) 75–82.

[19] M.H. Esfe, M. Afrand, S. Wongwises, A. Naderi, A. Asadi, S. Rostami, M. Akbari, Application of feedforward multilayer perceptron artificial neural networks and empirical correlation for prediction of thermal conductivity of $Mg(OH)_2$–EG using experimental data, Int. Commun. Heat Mass Transfer 67 (2015) (2015) 46–50.

[20] A.J. Litta, S.M. Idicula, U.C. Mohanty, Artificial neural network model in prediction of meteorological parameters during premonsoon thunderstorms, Int. J. Atmos. Sci. (2013) 1–14.

[21] S. Ballı, I. Tarımer, An application of artificial neural networks for prediction and comparison with statistical methods, Elektronika ir Elektrotechnika (Electron. Electr. Eng.) 10 (2) (2013) 101–105.

[22] Y.H. Hu, J.-N. Hwang, Handbook of Neural Network Signal Processing, CRC Press, Boca Raton, 2002.

[23] M.H. Beale, M.T. Hagan, B.D. Howard, 2011. Neural Network Toolbox™ 7. User Guide, R2011b.

[24] A.M. Aibinu, A.A. Shafie, M.J.E. Salami, Performance analysis of ANN based YCbCr skin detection algorithm, Procedia Eng. 41 (2012) 1183–1189.

[25] A.M. Aibinu, M.J.E. Salami, A.A. Shafie, Artificial neural network based autoregressive modeling techniques with application in voice activity detection, Eng. Appl. Artif. Intell. 25 (2012) 1255–1275.

Please cite this article in press as: J.O. Eichie et al., Artificial Neural Network model for the determination of GSM Rxlevel from atmospheric parameters, Eng. Sci. Tech., Int. J. (2016), http://dx.doi.org/10.1016/j.jestch.2016.11.002